




# Physico-mechanical properties of poly(ethylene glycol)-based polymer networks

Muhammad Humayun Bilal<sup>1</sup>  | Nasir Mahmood<sup>2</sup> |  
 Muhammad Haris Samiullah<sup>1</sup> | Karsten Busse<sup>1</sup>  | Jörg Kressler<sup>1</sup> 

<sup>1</sup>Institute of Chemistry,  
 von-Danckelmann-Platz 4, Martin Luther  
 University, Halle, Germany

<sup>2</sup>Institute of Physics,  
 Kurth-Mothes-Strasse 2, Martin Luther  
 University, Halle, Germany

## Correspondence

Jörg Kressler, Institute of Chemistry,  
 von-Danckelmann-Platz 4, Martin Luther  
 University, Halle 06120, Germany.  
 Email: [joerg.kressler@chemie.uni-halle.de](mailto:joerg.kressler@chemie.uni-halle.de)

## Funding information

Deutsche Forschungsgemeinschaft,  
 Grant/Award Number: KR 1714/9-2

## Abstract

Poly(ethylene glycol) (PEG) based networks have been used extensively for biomedical applications and as solid state electrolytes. In this work, a series of PEG networks was prepared using bifunctional PEG of molar mass 400, 1000, 2000, 4000, and 6000 g mol<sup>-1</sup> and star shaped PEG ( $M_n = 1000$  g mol<sup>-1</sup>) cross-linker using copper-catalyzed Huisgen 1,3-dipolar cycloaddition or “click” chemistry. The end-group modification of the bifunctional polymers and the star shaped cross-linker with alkyne and azide groups, respectively, was confirmed by <sup>1</sup>H NMR spectroscopy. The coupling reaction between azide and alkyne functionalities for the network formation was confirmed by Fourier transform infrared (FTIR) spectroscopy. The thermal properties of polymer network were determined by differential scanning calorimetry. Swelling studies of the networks were performed to correlate the network structure with the physical properties. The molar mass between the cross-links was determined using the Bray-Merill modified Flory-Rehner equation. The effect of molar mass between the cross-linking points on the strength of the networks was compared. Additionally, the effect of the stoichiometry of the precursors on the network strength was also studied. Finally, thickness-dependent tensile testing was performed to investigate the stress oscillation phenomenon.

## KEYWORDS

azide-alkyne click chemistry, mechanical properties, poly(ethylene glycol) networks, stress oscillation

## 1 | INTRODUCTION

Poly(ethylene glycol) based networks are among the most widely used polymeric materials with applications ranging from drug delivery system<sup>1,2</sup> and scaffolds for tissue engineering<sup>3-5</sup> to polymer electrolytes.<sup>6</sup> These materials

have been studied extensively for decades to investigate their properties for specific applications. Among the spectrum of properties of these polymer networks is their large deformation elasticity and swellability, mainly in water. The physical properties of cross-linked polymers are strongly dependent on the chemical structure and

This is an open access article under the terms of the [Creative Commons Attribution-NonCommercial-NoDerivs](https://creativecommons.org/licenses/by-nc-nd/4.0/) License, which permits use and distribution in any medium, provided the original work is properly cited, the use is non-commercial and no modifications or adaptations are made.

© 2023 The Authors. *Journal of Applied Polymer Science* published by Wiley Periodicals LLC.

homogeneity of the network.<sup>7</sup> Previously, different methods have been used to synthesize polymer networks.<sup>3,8–12</sup> However, these synthetic methods have some limitations, such as side reactions, uncontrolled reaction rates, and incomplete conversion which results in poorly defined networks with several defects, such as dangling chain ends, loops of different order, and entanglements. These kinds of defects certainly affect the mechanical and other properties of polymer networks. Similarly, it is very difficult to find the effect of cross-linker concentration on polymer networks synthesized by these methods.<sup>13</sup> Most recently, copper[I]-catalyzed 1,3 dipolar cycloaddition reaction (CuAAC) was used for the formation of 1,2,3-triazole junctions from azide and alkyne terminated PEG precursors (click chemistry) due of their high efficiency and selectivity.<sup>14–19</sup> This method produces polymer network with a high degree of cross-linking, small amounts of defects and structural inhomogeneities which results in improved mechanical properties.<sup>7,15,18–23</sup>

In the current study, three-arm star-shaped PEG azide was reacted with PEG- $\alpha,\omega$ -bis(alkyne) of different molar masses by CuAAC to investigate the effect of chain lengths of the precursors on the physical properties of the network. Thermal properties of the polymer network were determined by DSC measurement. The swellability of the polymer networks in water was quantitatively investigated using a modified Flory-Rehner based model.<sup>16,24</sup> Furthermore, the mechanical properties of all polymer networks synthesized were determined and compared with each other. In addition, the effect of sample thickness and the effect of stoichiometry on the mechanical response for the polymer networks were examined.

## 2 | MATERIALS AND METHODS

### 2.1 | Materials

For the syntheses of the precursors for network formation, three-arm glycerol ethoxylate ( $M_n = 1000 \text{ g Mol}^{-1}$ ), sodium hydride, calcium hydride, magnesium sulfate, methane sulfonyl chloride, triethylamine, anhydrous DMF, and sodium azide were purchased from Sigma-Aldrich and used as received.  $\alpha,\omega$ -dihydroxy poly(ethylene glycol) of molar mass 400, 1000, 2000, 4000 and  $6000 \text{ g Mol}^{-1}$  were purchased from Carl Roth. Propargyl bromide was received from abcr GmbH, while the solvents used for purification such as THF, ethyl acetate, n-hexane, methanol, and dichloromethane were purchased from VWR International. For the reaction, THF was dried over calcium hydride and freshly distilled before use. For synthesizing the polymer network,

$\text{CuSO}_4 \cdot 5\text{H}_2\text{O}$  and sodium ascorbate were purchased from Sigma Aldrich and deuterated solvents (deuterated DMSO- $d_6$  and  $\text{CDCl}_3$ ) from Armar AG.

### 2.2 | Methods

#### 2.2.1 | Synthesis of precursors of network

##### *Synthesis of star-shaped PEG-azide (PEG(S)-azide)*

For the synthesis of star-shaped PEG-azide, three-arm poly(ethylene glycol) (PEG(S)) was reacted with methane sulfonyl chloride followed by a reaction with sodium azide.<sup>18,25</sup> In a typical procedure, PEG (S) (15 g, 0.015 moles) was dissolved in 200 mL anhydrous THF in a 250 mL two-neck round bottom flask equipped with a magnetic stirrer and calcium chloride drying tube. The flask was placed in an ice bath and after 20 min trimethylamine (5.46 g, 0.054 moles) was added to the reaction flask. Then methane sulfonyl chloride (6.18 g, 0.054 moles) diluted with 20 mL anhydrous THF was added dropwise to the reaction mixture. The reaction mixture was stirred at  $0^\circ\text{C}$  for 2 h and then the reaction continued overnight at room temperature. At the end of the reaction, triethylammonium chloride was removed by filtration and the solvent was removed by a rotary evaporator at reduced pressure. The crude product was dissolved in dichloromethane (DCM) and extracted 3 times against 5% HCl, then three times against 5% NaOH and finally three times against brine. The organic phase was collected and dried over magnesium sulfate. DCM was removed by a rotary evaporator to obtain PEG(S)-mesyl as a yellowish liquid.

In the second step, PEG (S)-mesyl (10 g, 0.0081 moles) was added to a 250 mL two neck round bottom flask equipped with a heating plate, magnetic stirrer, and reflux condenser fitted with a calcium chloride drying tube. Then sodium azide (4.7 g, 0.0729 moles) and 200 mL DMF were added to the reaction flask. The reaction was allowed to proceed for 24 h at  $95^\circ\text{C}$ . After that, sodium salt was filtered off and DMF was evaporated using a rotary evaporator. The crude product was dissolved in DCM and extracted 3 times against the brine solution. The organic phase was removed on a rotary evaporator to obtain PEG (S)-azide as a pale yellow liquid. The  $^1\text{H}$  NMR spectrum of PEG (S)-azide is given in Figure S1 in the Supporting Information.

##### *Synthesis of linear PEG-alkyne*

PEG-alkyne of different molar masses was synthesized according to the procedure reported elsewhere.<sup>18,26</sup> In a typical experiment of PEG (1 k), weighted amount of sodium hydride (available as 60% dispersion in mineral

oil) (1.44 g, 0.036 moles) was dispersed in 150 mL anhydrous THF in a 500 mL two neck round bottom flask. The reaction flask was placed in an ice bath and stirred for 20 min. Then at 0°C, a mixture of PEG (1 k) (15 g, 0.015 moles) in 100 mL anhydrous THF was added with the help of a dropping funnel to the sodium hydride/THF mixture. The reaction mixture was stirred for 30 min at 0°C. Afterward, propargyl bromide (available as 80 wt% solutions in toluene) (5.8 g, 0.039 moles) diluted with 20 mL was added dropwise to the reaction mixture. The reaction was stirred again at 0°C for 2 h and then the reaction was continued overnight at room temperature. At the end of the reaction, a few drops of water were added to the reaction mixture to neutralize unreacted sodium hydride. The sodium bromide produced as side product during the reaction was removed by filtration. The solvent was removed under reduced pressure using a rotary evaporator and the synthesized crude product was dissolved in 200 mL dichloromethane and extracted three times against brine solution. The organic phase was collected and dried over magnesium sulfate. The mixture was concentrated on a rotary evaporator and the crude product was further purified by passing through silica column. Initially, an ethyl acetate and dichloromethane mixture (10:1 v/v) was used and later a dichloromethane and methanol mixture (10:1 v/v) was employed to collect the product.

Similarly, alkyne functionalization of different polymers, such as PEG (0.4 k), PEG (2 k), PEG (4 k), and PEG (6 k) were carried out. It is worth mentioning here that alkylnated PEG (2 k), PEG (4 k), and PEG (6 k) were purified by precipitation in diethyl ether instead of column chromatography. <sup>1</sup>H NMR spectra of alkyne functionalized PEG (0.4 k), PEG (1 k), PEG (2 k), PEG (4 k), and PEG (6 k) are shown in Figure S2 (Supporting Information).

### 2.2.2 | Network formation

Poly(ethylene glycol) networks were formed by coupling alkyne and azide functionalized PEG precursors via CuAAC reaction. Chemicals such as Cu[II]SO<sub>4</sub> and sodium ascorbate in water were used for the synthesis of polymer networks. In a typical experiment of PEG (S-1 k), PEG (S)-azide (1 g, 0.001 moles) along with PEG (1 k)-alkyne (1.5 g, 0.00139 moles) and CuSO<sub>4</sub>·5H<sub>2</sub>O (0.069 g, 0.000279 moles) were dissolved in 16 mL deionized water and stirred for a few min in a vial in order to make the reaction mixture homogeneous. Since the gelation time and final properties of the network depend on initial polymer concentration, all the PEG networks were

formed with an initial polymer concentration of 15% (w/v). Furthermore, sodium ascorbate (0.11 g, 0.000558 moles) dissolved in a small amount of water was added to the reaction vial and stirred for 1 to 1.5 min. After this, the reaction mixture was transferred to the mold and covered with a lid for 24 h. Then the cross-linked gel was removed from the mold and washed with ammonia solution for 7 to 10 days to remove the residual copper ions. For all these PEG polymer networks samples alkyne: azide = 1:1 (molar ratio) was used unless otherwise stated.

### 2.2.3 | Characterization

#### *Nuclear magnetic resonance spectroscopy*

Solution Nuclear magnetic resonance spectroscopy (NMR) spectra were recorded on a Varian Gemini 2000 operating at 400 MHz for <sup>1</sup>H NMR spectroscopy. Deuterated solvents like CDCl<sub>3</sub> and DMSO-d<sub>6</sub> were used for NMR spectroscopy. All the measurements were performed at 27°C.

#### *Attenuated total reflection-infrared spectroscopy*

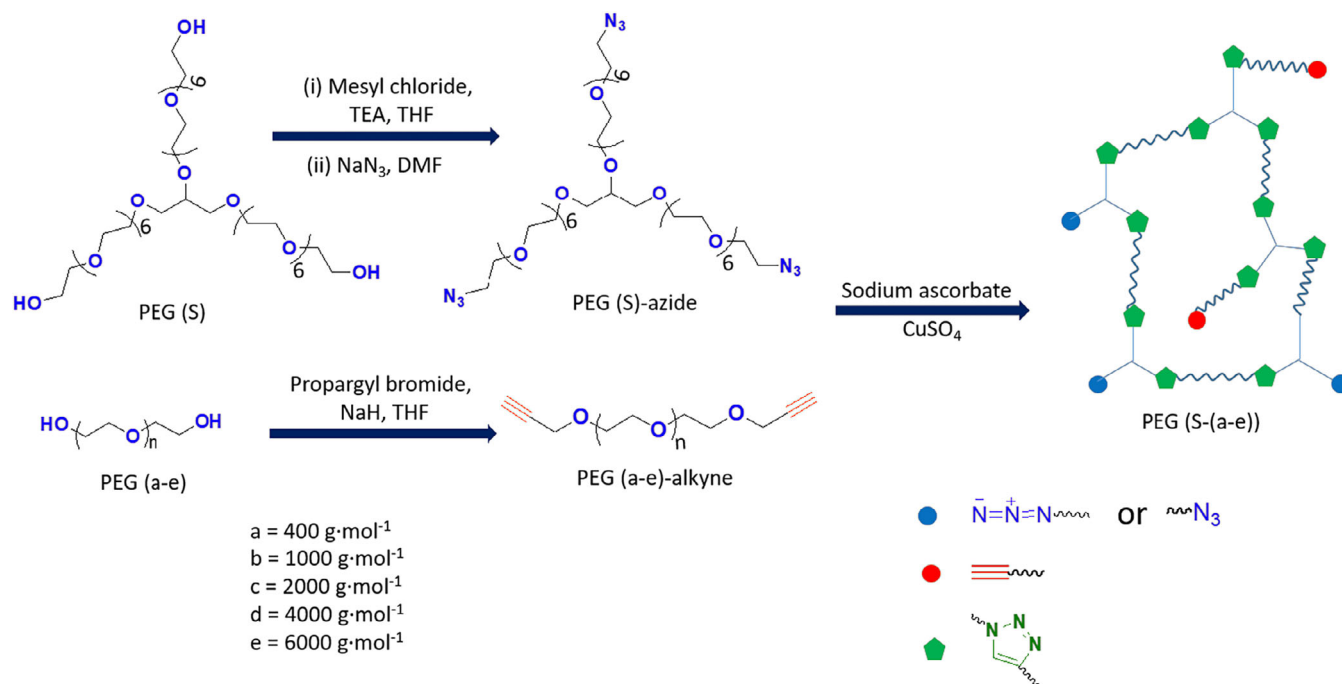
Attenuated total reflection-infrared spectroscopy (ATR-IR) measurements were carried on a Bruker Tensor BERTEX 70 equipped with a golden gate diamond ATR cell. For the analysis OPUS 6.5 software was used. All the measurements were carried out at room temperature and within the measurement range of 400 to 4000 cm<sup>-1</sup>. After cleaning the diamond crystal surface and measuring the background spectrum, both solid and liquid type samples were placed on top of the crystal surface. For each measurement, 16–32 scans were performed to obtain the final spectra depending upon the quality of the result obtained.

#### *Differential scanning calorimetry*

To investigate the thermal properties of polymer precursors and networks, differential scanning calorimetry (DSC) measurements were performed under nitrogen flow using a Mettler Toledo DSC 822e module. For this purpose, aluminum pans were filled with approximately 8–12 mg of sample. In case of PEG networks, samples were first heated to 120°C in order to remove the previous thermal history, and after holding this temperature for 10 min, they were cooled to -50°C at a rate of 5°C min<sup>-1</sup>. The samples were heated again to 80°C at 5°C min<sup>-1</sup>, to record their melting trace.

#### *Tensile testing*

Tensile tests were performed using a universal testing machine (Z010, Zwick/Roell) at room temperature and a testing speed of 27 mm·min<sup>-1</sup>. Dog-bone-shaped sample with a total length of 20 mm width of grip



**SCHEME 1** The overall synthesis route selected for the formation of PEG networks. [Color figure can be viewed at [wileyonlinelibrary.com](https://onlinelibrary.wiley.com)]

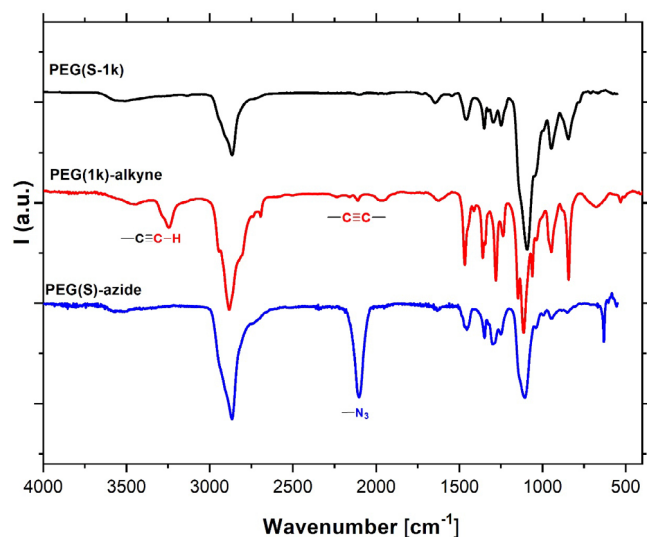


**FIGURE 1** FTIR spectra of PEG (S)-azide, PEG (1 k)-alkyne, and PEG (S-1 k). [Color figure can be viewed at [wileyonlinelibrary.com](https://onlinelibrary.wiley.com)]

section of 6 mm, a width of 2.02 mm, and a gage length of 12 mm was used for the measurement. Each measurement was repeated at least three times. Engineering stress and strain values were calculated based on force and displacement as well as initial specimen dimensions.

### 3 | RESULTS AND DISCUSSION

For network formation three-arm star shaped azide and bifunctional linear alkyne terminated PEGs (see Scheme 1) were successfully synthesized.  $^1\text{H}$  NMR spectra of all the azide and alkyne functionalized PEGs are given in Supporting Information as Figures S1 and S2. The integral values of alkyne functionalized PEGs are given in Table S1 in the Supporting Information.

Five PEG based polymer networks were synthesized using copper-catalyzed CuAAC as it is considered the best approach to achieve a controlled network formation, that would lead to better mechanical strength,<sup>27</sup> compared to polymer network synthesized for example, by photochemistry.<sup>8</sup> Fourier transform infrared spectroscopy (FTIR) was used to confirm the PEG polymer networks formation. Alkyne and azide functional groups have their unique band in FTIR spectra and these peaks disappeared as networks were formed. As an example, the FTIR spectra of PEG (1 k)-alkyne, PEG (S)-azide as well as their network are shown in Figure 1.

The PEG (1 k)-alkyne has two characteristic peaks at 2113 and  $3240 \text{ cm}^{-1}$  that belong to the stretching vibration of carbon atoms of the triple bond and stretching vibration of the terminal hydrogen and carbon atom of the alkyne functional group, respectively. In the case

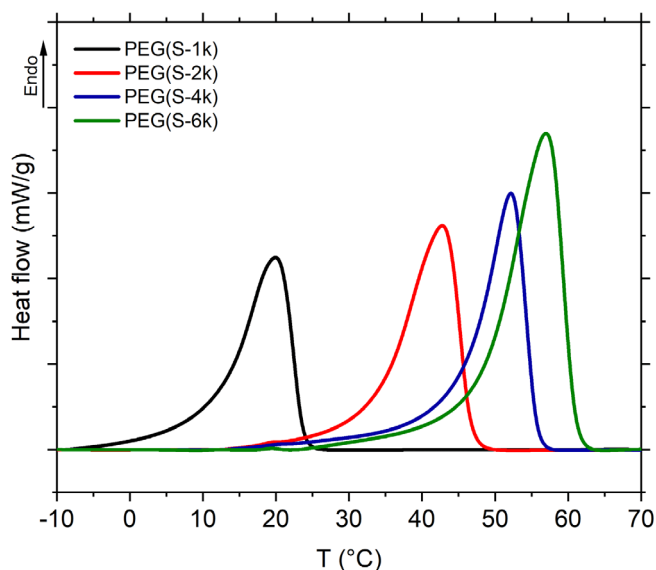


**FIGURE 2** DSC traces of PEG networks (PEG (S-1 k), PEG (S-2 k), PEG (S-4 k), and PEG (S-6 k), were obtained at a heating rate of 5°C/min. [Color figure can be viewed at [wileyonlinelibrary.com](http://wileyonlinelibrary.com)]

of PEG (S)-azide, the characteristic band appears at 2100  $\text{cm}^{-1}$  due to the stretching vibration of the azide functional group. However, in the network sample PEG (S-1 k) spectrum, the characteristic peaks of azide and alkyne functional groups disappeared completely, which indicates a high conversion within the detection limit of FTIR spectroscopy. The FTIR spectra of other network samples are given in Figures S3 to S6 in the Supporting Information.

### 3.1 | Thermal properties

The DSC measurements of all PEG network samples were carried out from  $-50$  to  $80^\circ\text{C}$  at a heating/cooling rate of  $5^\circ\text{C}/\text{min}$ . The DSC heating traces of the PEG networks are shown in Figure 2.

It was observed that all networks such as PEG (S-1 k), PEG (S-2 k), PEG (S-4 k), and PEG (S-6 k) are semi-crystalline as they show melting endotherms during the heating scan except PEG (S-0.4 k). The melting peaks of PEG networks are broad compared to linear PEG chains of corresponding molar mass.<sup>28</sup> As an example a comparison of DSC traces of linear PEG (2 k) and PEG (2 k) in the networks (named as PEG(S-2 k) is given in Figure S7 in the Supporting Information). Low melting temperature and broad peak indicate that PEG networks crystallize with relatively small lamellar thickness and have a large distribution of crystal size.<sup>28</sup> The crystallization data of PEG networks, such as melting temperature  $T_m$ , enthalpy of

melting  $\Delta H_m$ , and degree of crystallinity  $X_c$  are summarized in Table 1.

The degree of crystallinity  $X_c$  of all PEG networks is determined from the enthalpy of melting  $\Delta H_m$ , according to equation 1.

$$X_c = \frac{\Delta H_m}{\Delta H_m^0} \quad (1)$$

$\Delta H_m^0$  represents the enthalpy of melting of 100% crystalline PEG which is  $197\text{ J/g}$ .<sup>29</sup> The results given in Table 1 are in agreement with previous findings by Golitsyn et al.<sup>28</sup>

### 3.2 | Swelling measurements

The swelling of cross-linked polymer networks in the presence of a solvent is of significantly great theoretical and practical importance. Swollen polymer networks are termed as gels and can be applied for different applications such as membrane separation technology, biomedical applications and various physiological processes. When the dry polymer network gets in contact with suitable solvent molecules, the network's chains try to disperse or mix with the solvent molecules causing an increase in the system's entropy. However, stretching of network chains due to the swelling connected with volume expansion of the networks counterbalance this phenomenon. Similarly, strong solvent-polymer interactions and low cross-linking density favor the swelling process in the absence of other factors for example, pH-value of the solvent, temperature, presence of ionizable groups, and so forth.

For swelling experiments, vacuum dried weighed amount of PEG networks were soaked in deionized water for 24 h. To track the swelling process, samples were weighed after 1, 2, 4, 8, and 24 h, respectively (Figure 3).

The degree of swelling  $Q$  is defined as

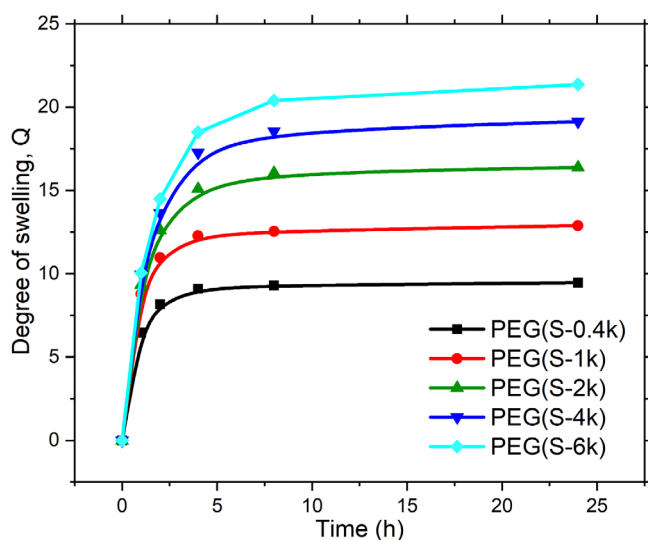
$$Q = \frac{m_s - m_d}{m_d} \quad (2)$$

Here,  $m_s$  is the mass of swollen network, whereas  $m_d$  stands for the mass of the dry network. Since PEG is a hydrophilic and water-soluble polymer, it is expected that PEG-based networks can absorb a huge amount of water and would behave like a hydrogel. For instance, PEG (S-0.4 k) can absorb water of about 9 times of its dry mass, whereas PEG (S-6 k) has water carrying capacity of 21 times of its dry mass.

The swelling phenomenon of polymer networks can be explained by the Flory-Rehner theory.<sup>30</sup> According to this theory, the thermodynamics of swelled polymer

TABLE 1 Melting temperature  $T_m$ , enthalpy of melting  $\Delta H_m$  and degree of crystallinity  $X_c$  of PEG networks obtained by DSC.

Sample	Melting temperature $T_m$ (°C)	Enthalpy of melting $\Delta H_m$ (J/g)	Degree of crystallinity $X_c$ (%)
PEG(S-1 k)	20	56.9	28.9
PEG(S-2 k)	42	70.2	35.6
PEG(S-4 k)	52	93.9	47.7
PEG(S-6 k)	57	98.1	50.0

FIGURE 3 Degree of swelling  $Q$  of PEG(S-0.4 k), PEG(S-1 k), PEG(S-2 k), PEG(S-4 k), and PEG(S-6 k) in water at 25°C. [Color figure can be viewed at [wileyonlinelibrary.com](http://wileyonlinelibrary.com)]

network is governed by two independent factors. The first factor is osmotic pressure  $\Pi_{mix}$ , which results from the polymer/solvent interaction and the other factor is the elastic pressure  $\Pi_{elas}$ , caused by the stretching of polymer chains between two cross-links. Hence, in the absence of any other contribution such as the presence of ionizable functional groups or  $pH$  variations, the elastic force balance between the osmotic pressure after a certain degree of swelling, and from the maximum allowed swelling values, one can get some basic understanding regarding the internal structure of networks (see Equation 3).

$$\Pi_{ext} = \Pi_{mix} - \Pi_{elas} \quad (3)$$

Here  $\Pi_{ext}$  represents any external pressure apart from osmotic and elastic forces and should be zero at equilibrium. The number of average molar mass between cross-links  $M_c$  can be calculated from the Bray-Merrill modified Flory-Rehner theory<sup>24,31</sup> for systems where the gelation process is conducted in solution.

$$\frac{1}{M_c} = \frac{2}{M_n} - \frac{\nu_1}{V_1} \frac{[\ln(1-\nu_2) + \nu_2 + \chi_{12}\nu_2^2]}{(\nu_2)^{\frac{1}{\phi}} - \left(\frac{2}{\phi}\right)\nu_2} \quad (4)$$

Here,  $\chi_{12}$  represents the polymer-solvent interaction parameter 0.426 for PEG in water,<sup>32,33</sup>  $V_1$  is the molar volume of water,  $\nu_1$  is the specific volume of polymer and  $\phi$  represents the functionality of the cross-linker (for the current system  $\phi = 3$ ).  $M_n$  Represents the average molar mass of linear chains between the two cross-links and this also includes the two adjacent arms of the cross-linker unit (molar mass of one arm of star shaped PEG cross-linker is 300 g mol<sup>-1</sup>). Thus for the PEG (S-1 k) network  $M_n$  is (300 + 1000 + 300 =) 1600 g mol<sup>-1</sup>. The equilibrium polymer volume fraction  $\nu_2$  which is the ratio of the dry gel and swollen gel volume can be calculated with the help of following equation.

$$\nu_2 = \frac{\rho_s}{Q\rho_p + \rho_s} \quad (5)$$

Here  $\rho_s$  represents the density of the solvent (water) and  $\rho_p$  is the density of the dry gel. In order to find the density of the network, the volume of the network was determined by immersing a weighed amount of a piece of the network in a flask containing n-hexane. As n-hexane is immiscible, the probability of an increase in the volume of the PEG network due to swelling is negligible. The increase in the volume of n-hexane due to the addition of the PEG networks was calculated and thus also the density. The values of average molar mass between the cross-links  $M_n$ , degree of swelling  $Q$ , the density of network  $\rho_p$  and molar mass between cross-links  $M_c$  of PEG(S-0.4 k), PEG (S-1 k), PEG (S-2 k), and PEG (S-6 k) are given in Table 2.

In an ideal network, the molar mass between the cross-links  $M_c$  calculated by the swelling experiments should be either equal to the theoretically expected values  $M_n$  or larger due to the presence of elastically inactive loops.<sup>18</sup> These loops do not contribute to the overall network formation process rather than extending the chain segments between two cross-links. However, in our PEG networks, the  $M_c$  values are almost 45% of that of the initial precursor  $M_n$ , indicating a cross-link density

**TABLE 2** Precursor molar mass  $\bar{M}_n$ , degree of swelling  $Q$ , the density of network  $\rho_p$  and molar mass between cross-links  $\bar{M}_c$  of PEG (S-0.4 k), PEG (S-1 k), PEG(S-2 k), and PEG (S-6 k) networks.

PEG networks	Average molar mass between the cross-links $\bar{M}_n$ (g Mol <sup>-1</sup> )	Density of network $\rho_p$ (g mL <sup>-1</sup> )	Degree of swelling $Q$	Molar mass between the cross-links $\bar{M}_c$ (g Mol <sup>-1</sup> )	$\frac{\bar{M}_c}{\bar{M}_n} \times 100$ (%)
PEG(S-0.4 k)	1000	0.73	9	443	44
PEG(S-1 k)	1600	0.76	13	731	46
PEG(S-2 k)	2600	0.79	16	1200	46
PEG(S-6 k)	6600	0.72	21	2838	43

much higher than expected for our system. These results are rather unexpected but are in agreement with the findings of Truong et al.<sup>16</sup> The  $\bar{M}_c$  values of their PEG networks were found to be about 50% of the theoretical value. The reason for this unexpected high cross-link density is that the pores in the networks become bigger with the increase in molar mass of the precursors due to the inherent heterogeneous network structure formed as a result of phase separation during the gelation process. Water is a relatively poor solvent for poly(ethylene glycol) as compared to alcohols and other chlorinated solvents and show both upper and lower critical solution temperature (UCST and LCST) behavior.<sup>34</sup> Moreover, it has been known that a critical concentration of PEG in water exists above which cluster formation occurs. These remain stable and they are in equilibrium with free polymer chains in water.<sup>34</sup> In our case as the network formation begins with the passage of time, the probability of an individually growing network structure reacting with other growing structures decreases, and the chances of intramolecular reaction with the same growing structure increases. This phenomenon introduces an inter-woven organization of chains entrapped in physical cross-links in the networks, which ultimately reduce the swelling and the degree of freedom of polymer chains.

### 3.3 | Tensile testing

The aim is to investigate the mechanical properties of polymer networks, and the effect of the length of network strands on mechanical properties. Network samples from linear PEG precursors of different molar masses of 0.4, 1, 2, 4, and 6 k g Mol<sup>-1</sup> with three-arm star PEG of 1 k were synthesized. All PEG networks are semi-crystalline, with the exception of the sample synthesized with the 0.4 k precursor, as indicated by the melting peaks during the heating scan in DSC measurements (as discussed before). The mechanical response of a semi-crystalline polymer network can thus be considered as a combination of stretching of the hard crystalline part and soft

amorphous part.<sup>35</sup> During the deformation of the specimen, the soft amorphous part act as a transmitter of entropic forces generated by the whole network. In literature, different mechanisms are proposed in order to explain the deformation of the semi-crystalline polymer networks. At low strain, the orientation of the amorphous chains along the drawing direction takes place that decreases the entropy of the amorphous phase resulting in a linear increase in stress with strain (Hookean elastic region). Upon further elongation of the sample, the yield point will be reached. About the yield point, there are two different arguments in the literature. First, the deformation was considered to be accomplished by inter-lamellar and intra-lamellar slips<sup>36–40</sup>; second, stress-induced melting and recrystallization were proposed to be responsible for the deformation process.<sup>41,42</sup> Further investigations revealed that both processes discussed above may be activated at different strains during tensile deformation.<sup>43</sup> Upon stretching, block slippage within the crystalline lamellae took place first, followed by a stress-induced fragmentation and recrystallization starting at a certain strain depending upon the stability of crystalline blocks and the state of the entangled amorphous network.<sup>36</sup> A higher entanglement density results in higher stress upon applied strain during deformation, whereas, the more stable the crystalline block, the higher the stress is needed for their destruction.<sup>36</sup> Upon such deformation the initial structure is transformed into a fibril structure, due to the preferential orientation of the molecular chains. Upon further stretching, the fibril structure becomes unstable resulting in cavitations accompanied by stretch-whitening.<sup>35</sup> At large strain, crystallization of amorphous chains occurs with a phenomenon called strain-induced crystallization which is also known for amorphous materials such as rubber.<sup>44,45</sup> In the case of PEG, during stress induce crystallization a point is reached where the crystal fraction tends to unity. This indicates that all the helical PEO chains have aligned along the deformation axis and are fully crystallized. Further deformation causes a transition of the network strands from helical into zigzag conformation.<sup>22</sup>

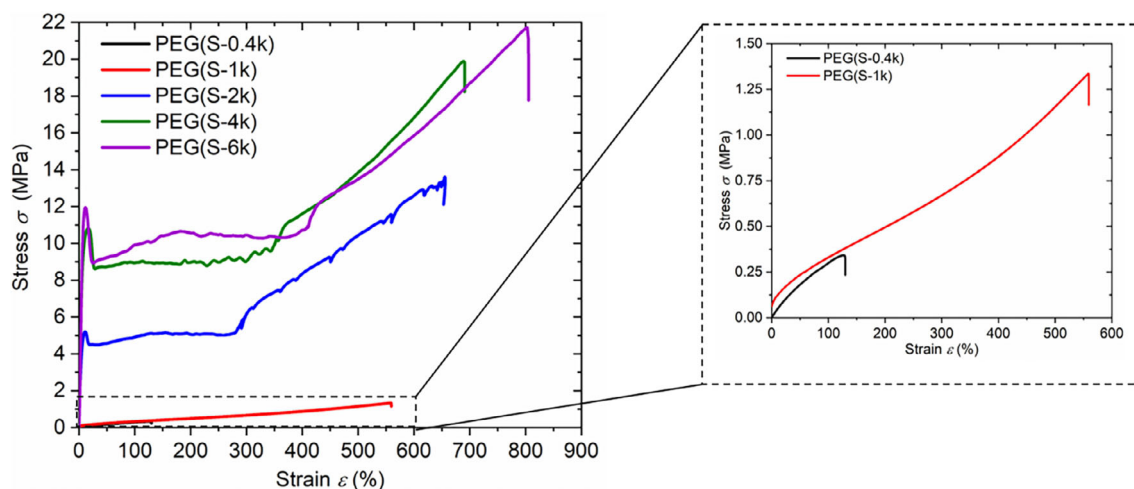


**FIGURE 4** Representative stress–strain curves of all network samples. The enlarged traces belong to PEG (S-0.4 k) and PEG (S-1 k). [Color figure can be viewed at [wileyonlinelibrary.com](http://wileyonlinelibrary.com)]

Figure 4 shows the stress–strain curves of the polymer network samples. It is observed that the network samples PEG (S-0.4 k) and PEG (S-1 k) have low modulus and tensile strength. The reason for this behavior is that they have a small distance between cross-links that reduce the elastic energy of the network and consequently result in low modulus and tensile strength. On the other hand, the network samples consisting of relatively high molar mass PEGs, such as PEG (S-2 k), PEG (S-4 k), and PEG (S-6 k) have high modulus and elongation at break. Furthermore, if the chain length of the PEGs is larger than the entanglement length of PEG of about  $2000 \text{ g Mol}^{-1}$  it is expected to have a high degree of entanglement which implies that a higher stress is generated upon applied strain when the sample is stretched.<sup>36,46</sup>

The initial crystallinity of the samples also plays an important role in determining the mechanical strength of the polymer networks.<sup>47</sup> It was observed that the sample with more initial crystallinity show high tensile strength or stress at break for example, PEG (S-2 k) ( $X_c = 35$ ,  $\sigma_B = 16.3 \pm 1.6 \text{ MPa}$ ), PEG(S-4 k) ( $X_c = 47$ ,  $\sigma_B = 17.5 \pm 3.3 \text{ MPa}$ ), and PEG (S-6 k) ( $X_c = 50$ ,  $\sigma_B = 20.68 \pm 1.03 \text{ MPa}$ ). This is because the presence of crystalline domains causes an additional resistance to deformation.<sup>20</sup> PEG (S-6 k) contains relatively large size crystals having more stability and regularity as compared to PEG (S-2 k) and PEG (S-1 k). This might be due to the decrease in the cross-linking density with the increase in chain length between two cross-links, which makes the PEG chains in the networks more mobile and flexible, allowing them to form bigger and more stable crystals. On the other hand, the samples PEG (S-0.4 k) and PEG (S-1 k) have a low stress at break of  $0.34 \pm 0.002$  and  $1.35 \pm 0.03$ , respectively.

This is due to the fact that the measurements were carried out above their melting temperatures. Therefore, under this condition they behave as amorphous networks. The complete mechanical data of all measured samples are given in Table 3.

In order to understand the effect of stoichiometry on the mechanical properties of the networks different species were prepared. Samples from PEG(S-2 k) were prepared with the following molar ratios [Azide]: [Alkyne]; 1.1: 1, 1: 1.1, 1: 1, 1: 1.05. The stress–strain curves of all these samples are given in Figure 5.

It was observed that the mechanical properties drastically deteriorate if stoichiometric conditions are broken. The decrease in mechanical strength of the network samples is due to strong inhomogeneity and defects (such as loop and dangling chain ends) in the sample.<sup>48</sup> The best networks are only obtained when equimolar alkyne and azide functional groups are used.

In the sample PEG(S-2 k) an unexpected serrated profile can be seen in the strain hardening region during neck propagation. This serrated profile is also termed stick-slip<sup>49–55</sup> or stress oscillation (SO) behavior.<sup>56–61</sup> Stress oscillation behavior is more commonly observed in metals,<sup>62</sup> however, this behavior has also been reported in various amorphous polymers such as poly(ethylene terephthalate) (PET)<sup>59,61,63–65</sup> as well as semi-crystalline polymers such as high-density polyethylene (HDPE),<sup>61,62</sup> isotactic polypropylene (iPP),<sup>62</sup> syndiotactic polypropylene (sPP),<sup>58,65</sup> and polyamides (PAs).<sup>62</sup> The mechanism of stress oscillation is still under debate as there are several disputes involved in the understanding the SO mechanism. Recently, Wan et al.<sup>66</sup> claim that the stress oscillation is the result of crazing and formation of microcavitation in poly(butylene succinate) specimens during



**TABLE 3** Mechanical characteristics of all network samples.  $E$  is the Young modulus,  $\sigma_Y$  is the stress at the yield point,  $\epsilon_Y$  is the strain at the yield point,  $\sigma_B$  is the stress at break, and  $\epsilon_B$  is the strain at break.

Sample	$E$ (MPa)	$\sigma_Y$ (MPa)	$\epsilon_Y$ (%)	$\sigma_B$ (MPa)	$\epsilon_B$ (%)
PEG(S-0.4 k)	$0.45 \pm 0.02$	–	–	$0.34 \pm 0.002$	$125 \pm 4.3$
PEG(S-1 k)	$25.5 \pm 0.8$	–	–	$1.35 \pm 0.03$	$535 \pm 38$
PEG(S-2 k)	$123 \pm 9$	$5.64 \pm 0.47$	$11.5 \pm 1.5$	$16.3 \pm 1.6$	$744 \pm 45$
PEG(S-4 k)	$152 \pm 12$	$10.2 \pm 0.84$	$15.2 \pm 0.25$	$17.5 \pm 3.3$	$656 \pm 56$
PEG(S-6 k)	$166 \pm 6$	$12.35 \pm 0.47$	$12.6 \pm 1.8$	$20.68 \pm 1.03$	$750 \pm 38$

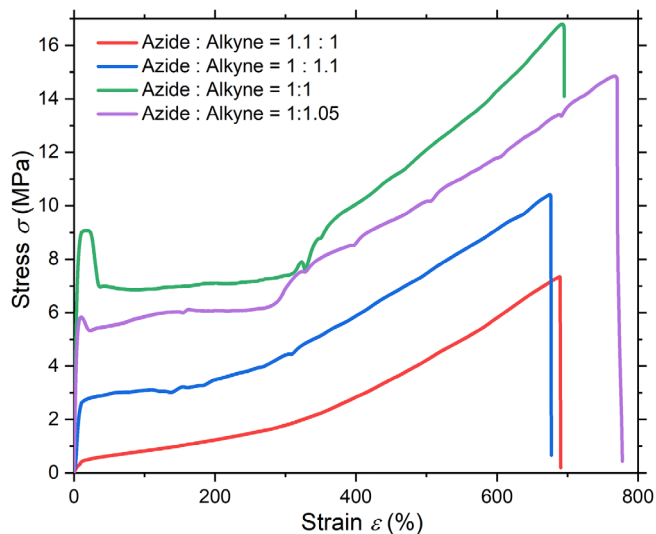


**FIGURE 5** Stress–strain curve of PEG (S-2 k) samples, obtained at different stoichiometric compositions of alkyne and azide functionalities. [Color figure can be viewed at [wileyonlinelibrary.com](http://wileyonlinelibrary.com)]

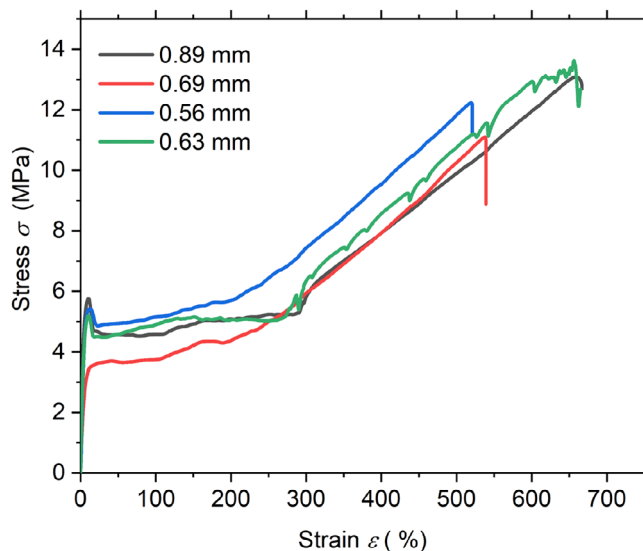


**FIGURE 6** Comparison of mechanical behavior of PEG(S-2 k) samples with different thicknesses. [Color figure can be viewed at [wileyonlinelibrary.com](http://wileyonlinelibrary.com)]

deformation. Cavity formation occurs simultaneously with the stress oscillation, periodically. Due to the cavity formation, the heat conductivity of the material decreases. This results in an increase in temperature of the deformation zone which weakens the polymer and causes the stress drop. During neck propagation, however, the material cools down, and the strength increases again, so the process becomes periodic. Years of investigation about understanding the SO mechanism shows that SO depends on the strain rate, specimen configuration (gauge length, thickness, and width), and material parameters (entanglements and network density). In this work, we have only studied the effect of thickness on the SO behavior of the sample keeping all other experimental parameters constant and observed that SO was only observed in sample that have a thickness of  $0.63 \pm 0.4$  mm. Thickness dependent tensile behavior of all the samples is shown in Figure 6.

This indicates that beside PEG (S-2 k) other PEG network samples studied in this work could also show SO under certain experimental conditions that can be further explored.

## 4 | CONCLUSION

In this study, well-defined poly(ethylene glycol) (PEG) based networks were synthesized using copper(I)-catalyzed azide-alkyne cycloaddition (CuAAC) “click” reaction by connecting linear dialkyne functionalized PEG oligomers and azide functionalized three-arm star shaped cross-linker. FTIR spectra of cross-linked networks show high conversion as the characteristic alkyne peaks at  $2113 \text{ cm}^{-1}$  (due to stretching vibration of carbon–carbon triple bond) and  $3240 \text{ cm}^{-1}$  (due to stretching vibration of terminal carbon-hydrogen bond) of bifunctional PEG and stretching vibration of azide group of cross-linker at  $2100 \text{ cm}^{-1}$  are absent. DSC studies show a decrease in the melting temperature, increase in melting peak width, and decrease in crystallinity of the PEG networks compared to the corresponding linear polymers. This proves that PEG networks crystallize with small lamellar thickness and have a large distribution of crystal size. It also validates the point that cross-linked polymer networks tend to have lower crystallinity as compared to the native form of the polymer precursors

because of the hindrance in the degree of freedom of polymers.<sup>28</sup> From the swelling experiment, it was found that the swellability of the network is directly related to the molar mass of the linear PEG precursors used for its formation. For instance, PEG (S-0.4 k) can absorb water 9 times its dry mass, whereas PEG (S-6 k) can carry water 21 times its dry mass. PEG networks obtained from the high molar mass are more promising materials as they have larger pore sizes or cavities that could be useful for the diffusion of ions and other solutes. Tensile testing of network samples shows that the network consisting of relatively high molar mass PEGs such as PEG (S-2 k), PEG (S-4 k), and PEG (S-6 k) have high modulus and strength at break. This could be related to the initial crystallinity of the sample, that is, the higher the crystallinity of the samples the higher will be its strength at break for example, PEG (S-2 k) ( $X_c = 35$ ,  $\sigma_B = 16.3 \pm 1.6$  MPa) and PEG (S-6 k) ( $X_c = 50$ ,  $\sigma_B = 20.68 \pm 1.03$  MPa). Here, the crystal domains cause an additional resistance to deformation. Hence, we can say that the increase in the molar mass of PEG-based precursors is directly proportional to the increase in crystallinity and higher mechanical strength. It was also observed from thickness-dependent tensile measurements that the stress oscillation phenomenon during strain hardening could be a material property but it is strongly dependent on the thickness of the samples. Based upon the findings of PEG-based networks' characterization data, it can be assumed that the networks comprised of high molar mass PEG precursors are deemed more suitable for the desired applications, such as electrochemical devices and drug release systems.

### AUTHOR CONTRIBUTIONS

**Jörg Kressler:** Conceptualization (lead); funding acquisition (lead); project administration (lead); supervision (lead); writing – review and editing (lead). **Muhammad Humayun Bilal:** Conceptualization (lead); formal analysis (lead); methodology (lead); software (lead); writing – original draft (lead). **Nasir Mahmood:** Data curation (supporting); formal analysis (supporting); methodology (supporting); writing – review and editing (supporting). **Muhammad Haris Samiullah:** Conceptualization (supporting); formal analysis (supporting); investigation (supporting); methodology (supporting); writing – review and editing (supporting). **Karsten Busse:** Conceptualization (supporting); data curation (supporting); formal analysis (supporting); methodology (supporting); writing – review and editing (supporting).

### ACKNOWLEDGMENTS

The authors gratefully acknowledge financial support from Deutsche Forschungsgemeinschaft (DFG) project

KR 1714/9-2. The authors would also like to thank to research group of Prof. Wolfgang H. Binder, Department of Chemistry, Martin-Luther University Halle-Wittenberg, Germany for performing IR measurements. Open Access funding enabled and organized by Projekt DEAL.

### CONFLICT OF INTEREST STATEMENT

The authors declare no conflicts of interest.

### DATA AVAILABILITY STATEMENT

The data that support the findings of this study are available from the corresponding author upon reasonable request.

### ORCID

Muhammad Humayun Bilal  <https://orcid.org/0000-0001-5887-1536>

Karsten Busse  <https://orcid.org/0000-0003-4168-0957>

Jörg Kressler  <https://orcid.org/0000-0001-8571-5985>

### REFERENCES

- [1] C. C. Lin, A. T. Metters, *Adv. Drug Deliv. Rev.* **2006**, *58*, 1379.
- [2] I. Gibas, H. Janik, *Chem. Chem. Technol.* **2010**, *4*, 297.
- [3] K. T. Nguyen, J. L. West, *Biomaterials* **2002**, *23*, 4307.
- [4] J. A. Burdick, K. S. Anseth, *Biomaterials* **2002**, *23*, 4315.
- [5] E. S. Place, J. H. George, C. K. Williams, M. M. Stevens, *Chem. Soc. Rev.* **2009**, *38*, 1139.
- [6] N. Hasan, M. Pulst, M. H. Samiullah, J. Kressler, *J. Polym. Sci. B Polym. Phys* **2019**, *57*, 21.
- [7] M. Tosa, K. Hashimoto, H. Kokubo, K. Ueno, M. Watanabe, *Soft Matter* **2020**, *16*, 4290.
- [8] T. S. Hebner, H. E. Fowler, K. M. Herbert, N. P. Skillin, C. N. Bowman, T. J. White, *Macromolecules* **2021**, *54*, 11074.
- [9] H. Rashid, Y. Golitsyn, M. H. Bilal, K. Mäder, D. Reichert, J. Kressler, *Gels* **2021**, *7*, 1.
- [10] R. Alaneed, Y. Golitsyn, T. Hauenschild, M. Pietzsch, D. Reichert, J. Kressler, *Polym. Int.* **2021**, *70*, 135.
- [11] S. Lin-Gibson, R. L. Jones, N. R. Washburn, F. Horkay, *Macromolecules* **2005**, *38*, 2897.
- [12] E. M. Ahmed, *J. Adv. Res.* **2015**, *6*, 105.
- [13] A. Sugimura, M. Asai, T. Matsunaga, Y. Akagi, T. Sakai, H. Noguchi, M. Shibayama, *Polym. J.* **2013**, *45*, 300.
- [14] K. Oshima, T. Fujimoto, E. Minami, Y. Mitsukami, *Macromolecules* **2014**, *47*, 7573.
- [15] K. Li, C. Zhou, S. Liu, F. Yao, G. Fu, L. Xu, *React. Funct. Polym.* **2017**, *117*, 81.
- [16] V. Truong, I. Blakey, A. K. Whittaker, *Biomacromolecules* **2012**, *13*, 4012.
- [17] X. Ding Tao, G. Yuanqing, J. Huang, L. Yurong, F. Xiaomin, Z. Liqun, *J. Appl. Polym. Sci.* **2010**, *118*, 2442.
- [18] M. H. Samiullah, D. Reichert, T. Zinkevich, J. Kressler, *Macromolecules* **2013**, *46*, 6922.
- [19] M. Shibayama, X. Li, T. Sakai, *Colloid Polym. Sci.* **2019**, *297*, 1.
- [20] C. B. Zhang, L. Wang, B. Yang, H. Zhao, G. M. Liu, D. J. Wang, *Chinese J. Polym. Sci.* **2022**, *40*, 256.

- [21] A. K. Zhang, J. Ling, K. Li, G. D. Fu, T. Nakajima, T. Nonoyama, T. Kurokawa, J. P. Gong, *J. Polym. Sci. B Polym. Phys.* **2016**, *54*, 1227.
- [22] E. Wang, F. A. Escobedo, *Macromolecules* **2016**, *49*, 2375.
- [23] T. Sakai, T. Matsunaga, Y. Yamamoto, C. Ito, R. Yoshida, S. Suzuki, N. Sasaki, M. Shibayama, U. Chung, *Macromolecules* **2008**, *41*, 5379.
- [24] K. B. Keys, F. M. Andreopoulos, N. A. Peppas, *Macromolecules* **1998**, *31*, 8149.
- [25] J. Edward Semple, B. Sullivan, T. Vojtkovsky, K. N. Sill, *J. Polym. Sci. A Polym. Chem.* **2016**, *54*, 2888.
- [26] M. Van Dijk, C. F. Van Nostrum, W. E. Hennink, D. T. S. Rijkers, R. M. J. Liskamp, *Biomacromolecules* **2010**, *11*, 1608.
- [27] M. Malkoch, R. Vestberg, N. Gupta, L. Mespouille, P. Dubois, A. F. Mason, J. L. Hedrick, Q. Liao, C. W. Frank, K. Kingsbury, C. J. Hawker, *Chem. Commun.* **2006**, *26*, 2774.
- [28] Y. Golitsyn, M. Pulst, M. H. Samiullah, K. Busse, J. Kressler, D. Reichert, *Polymer* **2019**, *165*, 72.
- [29] C. P. Buckley, A. J. Kovacs, *Colloid Polym. Sci.* **1976**, *254*, 695.
- [30] P. J. Flory, J. Rehner, *J. Chem. Phys.* **1943**, *11*, 512.
- [31] J. C. Bray, E. W. Merrill, *J. Appl. Polym. Sci.* **1973**, *17*, 3779.
- [32] E. W. Merrill, K. A. Dennison, C. Sung, *Biomaterials* **1993**, *14*, 1117.
- [33] U. Akalp, S. Chu, S. C. Skaalure, S. J. Bryant, A. Doostan, F. J. Vernerey, *Polymer* **2015**, *66*, 135.
- [34] C. Özdemir, A. Güner, *Eur. Polym. J.* **2007**, *43*, 3068.
- [35] Y. Men, *Macromolecules* **2020**, *53*, 9155.
- [36] Y. Men, J. Rieger, G. Strobl, *Phys. Rev. Lett.* **2003**, *91*, 1.
- [37] L. Iannucci, S. Del Rosso, P. T. Curtis, D. J. Pope, P. W. Duke, *Materials* **2018**, *11*, 11.
- [38] S. Fateh Ali, J. Fan, *J. Mater. Sci. Technol.* **2020**, *57*, 12.
- [39] Y. Nie, H. Gao, W. Hu, *Polymer* **2014**, *55*, 1267.
- [40] Q. Chen, H. Chen, L. Zhu, J. Zheng, *J. Mater. Chem. B* **2015**, *3*, 3654.
- [41] D. Y. Yoon, P. J. Flory, *Faraday Discuss. Chem. Soc.* **1979**, *68*, 288.
- [42] W. Wu, G. D. Wignall, L. Mandelkern, *Polymer* **1992**, *33*, 4137.
- [43] Y. Men, J. Rieger, K. Hong, *J. Polym. Sci. B Polym. Phys.* **2005**, *43*, 87.
- [44] S. Xu, J. Zhou, P. Pan, *Macromol. Chem. Phys.* **2022**, *223*, 1.
- [45] S. Toki, T. Fujimaki, M. Okuyama, *Polymer* **2000**, *41*, 5423.
- [46] S. Jabbari-Farouji, O. Lame, M. Perez, J. Rottler, J. L. Barrat, *Phys. Rev. Lett.* **2017**, *118*, 1.
- [47] C. Qian, Y. Zhao, Y. Wang, C. Zhang, D. Wang, *Polymer* **2021**, *236*, 124310.
- [48] T. Matsunaga, H. Asai, Y. Akagi, T. Sakai, U. Chung, M. Shibayama, *Macromolecules* **2011**, *44*, 1203.
- [49] C. Creton, M. Ciccotti, *Reports Prog. Phys.* **2016**, *79*, 46601.
- [50] J. J. Scavuzzo, X. Yan, Y. Zhao, J. D. Scherger, J. Chen, S. Zhang, H. Liu, M. Gao, T. Li, X. Zhao, G. R. Hamed, M. D. Foster, L. Jia, *Macromolecules* **2016**, *49*, 2688.
- [51] C. Zhang, S. Ketten, D. Derome, J. Carmeliet, *Carbohydr. Polym.* **2021**, *258*, 117682.
- [52] C. Dong, C. Yuan, X. Bai, H. Qin, X. Yan, *Wear* **2017**, *376–377*, 1333.
- [53] K. Viswanathan, N. K. Sundaram, *Wear* **2017**, *376–377*, 1271.
- [54] S. Liu, R. Maheshwari, K. L. Kiick, *Macromolecules* **2009**, *42*, 3.
- [55] M. Liu, J. Sun, Y. Sun, C. Bock, Q. Chen, *J. Micromech. Microeng.* **2009**, *19*, 19.
- [56] A. Toda, *Polymer* **1993**, *34*, 2306.
- [57] Q. Jiao, J. Shen, L. Ye, Y. Li, H. Chen, *Polymer* **2019**, *167*, 40.
- [58] M. C. García Gutiérrez, J. Karger-Kocsis, C. Riekel, *Chem. Phys. Lett.* **2004**, *398*, 6.
- [59] A. Toda, C. Tomita, M. Hikosaka, Y. Hibino, H. Miyaji, C. Nonomura, T. Suzuki, H. Ishihara, *Polymer* **2001**, *43*, 947.
- [60] I. W. Moran, S. B. Jhaveri, K. R. Carter, *Small* **2008**, *4*, 1176.
- [61] G. P. Andrianova, A. S. Kecheqyan, V. A. Kargin, *J. Polym. Sci. A-2 Polym. Phys.* **1971**, *9*, 1919.
- [62] B. M. Lipinski, L. S. Morris, M. N. Silberstein, G. W. Coates, *J. Am. Chem. Soc.* **2020**, *142*, 6800.
- [63] R. Roseen, *J. Mater. Sci.* **1974**, *9*, 929.
- [64] F. Ronkay, T. Czigány, *Polym. Bull.* **2006**, *57*, 989.
- [65] H. Ebener, B. Pleuger, J. Petermann, *J. Appl. Polym. Sci.* **1999**, *71*, 813.
- [66] C. Wan, E. L. Heeley, Y. Zhou, S. Wang, C. T. Cafolla, E. M. Crabb, D. J. Hughes, *Soft Matter* **2018**, *14*, 9175.

## SUPPORTING INFORMATION

Additional supporting information can be found online in the Supporting Information section at the end of this article.

**How to cite this article:** M. H. Bilal, N. Mahmood, M. H. Samiullah, K. Busse, J. Kressler, *J. Appl. Polym. Sci.* **2023**, *140*(48), e54726. <https://doi.org/10.1002/app.54726>